

# Hardware-in-the-loop performance analysis of a railway traction system under sensor faults

eISSN 2051-3305

Received on 26th June 2018

Accepted on 31st July 2018

E-First on 21st May 2019

doi: 10.1049/joe.2018.8249

www.ietdl.org

Fernando Garramiola<sup>1</sup> ✉, Javier Poza<sup>1</sup>, Jon del Olmo<sup>1</sup>, Txomin Nieva<sup>2</sup>

<sup>1</sup>Electronics and Computer Science Department, Faculty of Engineering, Mondragon Unibertsitatea, Spain

<sup>2</sup>CAF Power & Automation, Spain

✉ E-mail: fgarramiola@mondragon.edu

**Abstract:** Fault mode and effects analysis (FMEA) has been used during decades for analysing the effects of faults in different applications. Initially, FMEA based on risk priority numbers provided information about the effects in the system, but during the last years different approaches have been developed to obtain a more robust risk evaluation. The proposed enhanced FMEA can provide the quantitative effects of sensor faults in a railway traction drive, in variables such as torque, current and voltages. In addition to the previous work, quantitative effects on overall performance indicators, such as energy efficiency and comfort, are obtained too. Hardware-in-the-loop (HIL)-based fault injection approach has been used to generate fault scenarios. The test platform is composed of a real-time simulator and a commercial traction control unit for a railway application.

## 1 Introduction

An increasing demand for higher performance and cost-effectiveness has stimulated the development of measures to increase the system safety and reliability in industry. Furthermore, in traction systems, such as railway applications, a higher system availability has become a compulsory key element for market competition.

Thus, dependability analysis is needed to manage the faults, their effects and propagation, and in consequence, the risks of the system. Original failure mode and effect analysis (FMEA) and fault tree analysis (FTA) are some of the most important qualitative dependability analysis approaches.

In [1], an improved FMEA for rail and automotive industry is presented, based on risk priority numbers (RPNs). Later, FMEA methodology has been spread to other industries [2, 3]. RPN is a probability value presented in terms of severity, occurrence and detection ratings. Due to the shortcomings of RPN, further publications [4] have proposed enhanced approaches to provide a quantitative value for FMEA.

Moreover, advances in automation and monitoring have allowed the fusion of FMEA and measured data [5], generating an adaptive FMEA during the system life cycle, providing reliable quantitative information to maintenance managers.

The need of integration of dependability analysis and enhanced FMEA [6] in the maintenance process beyond the design phase has been previously mentioned, as a barrier not already solved. Moreover, the methodology to generate the enhanced FMEA was also presented by the author.

Once a fault occurs, system performance deteriorates from the nominal zone to the degraded zone. Moreover, the fault can generate a safety risk, leaving the safety zone, and protections act to avoid a failure. Based on fault injection procedure, information to set the bounds of the degraded and safety zones can be obtained, as well as the levels of performance inside the degraded zone.

Recently, the fault-injection approach [7] has been used to analyse some fault scenarios, but not with the idea to generate an enhanced FMEA.

A hardware-in-the-loop (HIL) platform has been used for sensor fault injection. HIL approach is already utilised for different applications, such as control software development or system performance validation [8]. It allows using models instead of hardware, which reduces cost in complex test systems. In [9], the HIL approach is presented as a previous step to the final testing of a fault diagnosis system, based on a V Model development.

The aim of the proposed article is to present the quantitative effects of sensor faults, on the traction drive performance, based on fault-injection approach and HIL platform. Quantitative effects are obtained for all the sensor fault modes defined by traction drive manufacturer. The level of performance is monitored and compared with the quantitative effects in degraded mode, previously obtained during fault injection and HIL simulation, and as result, a fault mode can be early detected and diagnosed. Moreover, the more suitable actions to improve the availability of the traction unit can be proposed.

The case study for the application of the proposed approach is a traction unit of a railway application. Different levels of performance will be provided for all the current and voltage sensor fault modes in a railway traction unit, so a complete enhanced FMEA for sensor faults will be provided. Despite the fact that the information is obtained for a railway application, the methodology and classification structure could be applied to other applications.

The HIL platform is composed of a real-time simulator and a traction control unit (TCU) for a Railway application. The TCU is a commercial unit for a tram develop by CAF Power & Automation (CAF P&A).

The paper is organised as follows. Section 2 presents the system under analysis, the initial FMEA and the platform used. Section 3 shows system performance under sensor faults. In Section 4, the enhanced FMEA for the system analysed is presented. Finally, conclusions are drawn in Section 5.

## 2 Tools for model based analysis for railway traction units

The traction unit analysed in this paper was designed for a tram. As it can be seen in Fig. 1, the traction unit is composed by the TCU, the input filter, the braking chopper and the inverter for supplying two motors in parallel.

The TCU includes the control strategy implemented for the real application. The torque and flux control strategy is divided in four control modes depending on the motor speed. Some of the functionalities of the TCU are the control strategies for the inverter and chopper, set-point generation, protections and alarms management.

Before starting the model-based analysis, a HIL platform to inject faults and an initial FMEA, based on information from the manufacturer are needed. The goal of the HIL platform is to inject faults and analyse the effects on the system. The faults to inject are defined by the initial FMEA, which provides the usual faults in the

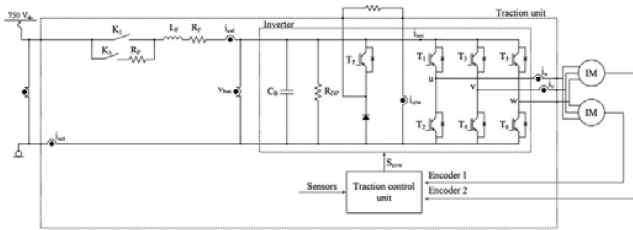


Fig. 1 Railway traction unit

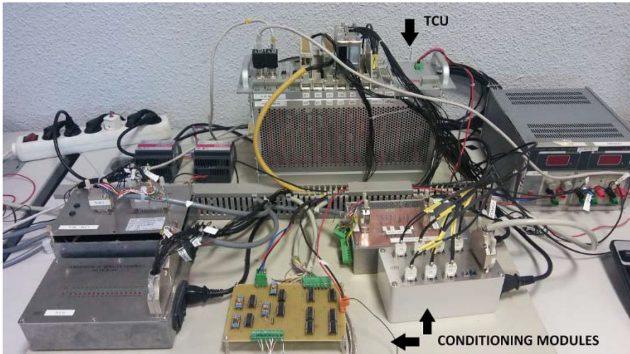


Fig. 2 TCU and conditioning modules of HIL platform

system rated by severity, occurrence and detection. This tool allows to prioritise the faults to analyse.

The methodology to obtain the enhanced FMEA has the following steps:

- (i) Collect the initial FMEA and the model used during design phase.
- (ii) Plan the test to take place in the HIL platform
- (iii) Develop an extended model to allow fault injection
- (iv) Execute the test in HIL platform
- (v) Evaluate the results and enhance the initial FMEA.

In this section, the resources needed by the methodology to enhance the FMEA [10] will be described.

### 2.1 HIL platform

The traction unit, with the exception of TCU, and the machines are modelled in MATLAB-Simulink. This allows adapting the configuration to different traction units quickly, as normally the changes are related to the number of branches of the input filter, the number of motors and the number of inverters. In previous research works [11, 12], and in collaboration with CAF P&A, the models have validated with experimental data. The traction unit models developed during the design phase can be reused during the fault-injection phase.

The traction unit model runs in a real-time simulator from OPAL-RT Company. A real-time simulator uses a fixed step solver, so the simulator should do the calculations inside that time interval, to present the result at the end of the interval. Thus, the simulation time is equal to the real time needed by the system.

The TCU is externally connected to the real-time simulator. Conditioning modules to adapt the I/O between TCU and real-time simulator are needed, as it is shown in Fig. 2. The sensor fault modes are generated in MATLAB-Simulink and injected into the TCU inputs. This platform allows injecting faults and analysing the effects easily and quickly.

### 2.2 FMEA

During the system design phase an initial FMEA is defined. This information was provided by CAF P&A. The FMEA includes the component analysed, the fault description and its effects, and finally the way to detect it. The FMEA is normally referred to the safety zone, and it does not take into account the degraded zone. The limits of the safety zone are usually set without taking into

account the system performance, and in consequence, it can decrease the availability of the system. As an example, a reduced FMEA for the DC-link voltage sensor and one fault mode is presented in Table 1. No maintenance action is taken until failure occurs.

Opposed to the initial FMEA, a quantitative FMEA like the one proposed in Section 4, can provide information about a fault mode in the degraded zone, so a maintenance action can be performed to avoid a failure. It opens to new maintenance strategy options, as condition-based maintenance (CBM), already studied in railway applications [13].

Moreover, a quantitative FMEA can provide more reliable information to set the limits of the safety zone, which could increase the availability of the system.

## 3 System performance under sensor faults

Based on [14] and information from the initial FMEA, more relevant sensor faults have been injected to voltage and current sensors: bias (constant offset), drift (time varying offset), gain. Hard faults (e.g. lack of sensor measurement) have not been analysed, as they produce a failure, and the goal of this analysis is the identification of the performance in the degraded zone.

The system performance test should be planned in order to represent a real scenario. The test plan should include the working point, fault mode, and system configuration. Furthermore, the expected effects from FMEA should be taken into account, as indicators to analyse.

Due to the relevance in system performance, phase current sensors and DC-link voltage sensors were prioritized. The DC-link voltage sensor is represented as  $v_{bus}$  in Fig. 1, whereas phase current sensors are represented as  $i_u$  and  $i_v$ . Thus, gain faults in  $v_{bus}$  sensor and  $i_u$  sensors are presented here, analysing their influence in the system energy efficiency and comfort, respectively. In the same way, the methodology was applied to the other sensors.

In [15] it was shown that an offset fault in the phase current sensor of an AC motor results in a oscillation in the torque at a frequency  $f_s$ , being  $f_s$  the fundamental frequency of motor supply, whereas a gain fault results in a oscillation of twice  $f_s$ . It is important to mention that a faulty connection of any of the motor cables will generate a similar oscillation. Thus, a gain fault in one of the phase current sensors ( $i_u$ ) was injected, so the effects on the torque and the jerk in steady state can be analysed.

If a phase current sensor measures a higher value than the real one, the estimated torque will be higher too, so the control strategy will adapt the estimated torque to the reference torque, as a consequence the real torque will be lower than in the fault-free case, as it is shown in Fig. 3, for maximum torque reference. Furthermore, this implies that more time is needed to reach the desired speed and to travel a distance, as it is shown in Table 2. In case of a faulty sensor, measuring a lower value than the real one, the effects will be the opposite ones. The allowed maximum torque is not reached, increasing the power consumed to travel the same distance.

Furthermore, the oscillation due to a faulty phase current sensor can affect to the comfort of the train. Comfort is related to low frequencies in traction applications, from 1 to 80 Hz [16]. Thus, given a reference for the motor mechanical frequency  $f_m$  equal to 20 Hz, equivalent to 600 rpm, in Fig. 4 can be seen that the jerk value for twice the electrical frequency of the motor increases. In order to analyse the same working point (torque and speed), the reference torque has been increased in the faulty case. Depending on the system, the oscillation could generate a low frequency vibration in the train. The EN 13452-1:2003 standard [17] limits the maximum jerk in service to  $1.5 \text{ m/s}^3$  in railway applications.

On the other hand, DC-link voltage sensor faults were analysed. Similar to the previous case, an example for one fault mode is presented. The case proposed here shows a gain deviation in the sensor, measuring a higher voltage than the real one. In this case, the energy efficiency of the system is affected, because the braking chopper starts working earlier to avoid an overvoltage. Thus, more energy is dissipated in the braking resistor instead of returning it to

**Table 1** Reduced FMEA for DC-link voltage sensor

Sensor	Fault mode	Cause	System effect	Detection
sensor $v_{bus}$	measured value higher than real one	sensor fault	DC-link not charged and inverter disabled	safety maximum DC-link voltage

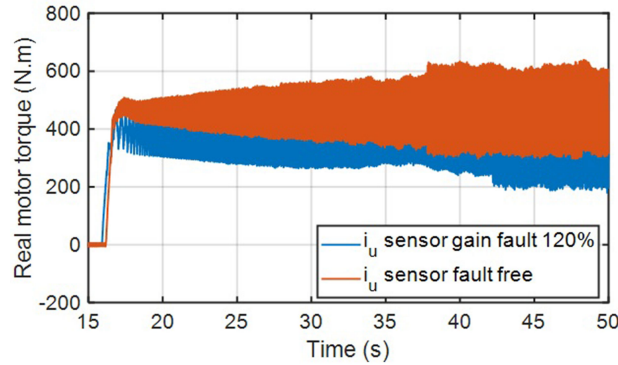


**Fig. 3** Comparison of real motor torque during acceleration for current sensor faulty and fault-free cases

**Table 2** Travel performance analysis for current sensor gain fault

	$i_u$ gain fault 110%	$i_u$ gain fault 120%	$i_u$ gain fault 140%
percentage of time increment from fault free case for travelling 400 m at maximum reference torque	3%	9%	16%
percentage of torque deviation in steady state referred to maximum torque per machine 460 N m in control mode 1 (600 rpm)	-9.6%	-18.4%	-29.3%

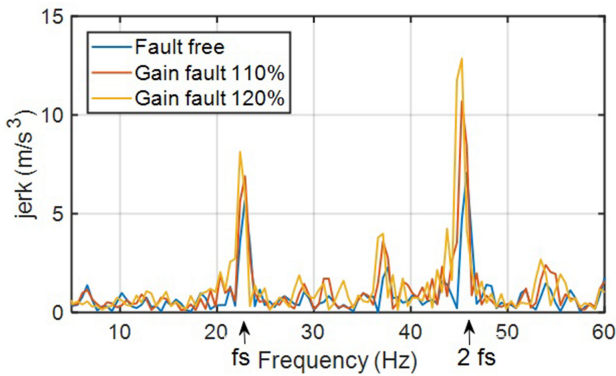


**Fig. 4** Spectrum of jerk for fault free and  $i_u$  sensor faulty

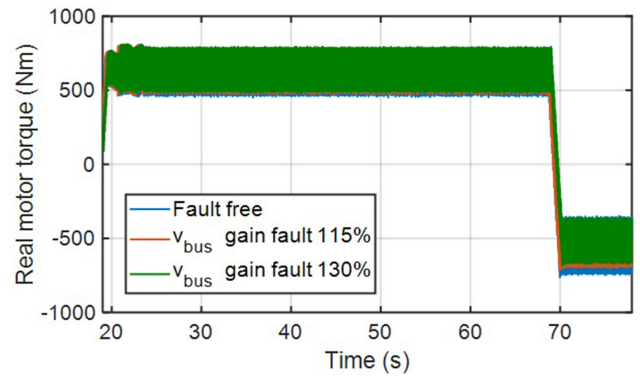


**Fig. 6** Real torque per motor

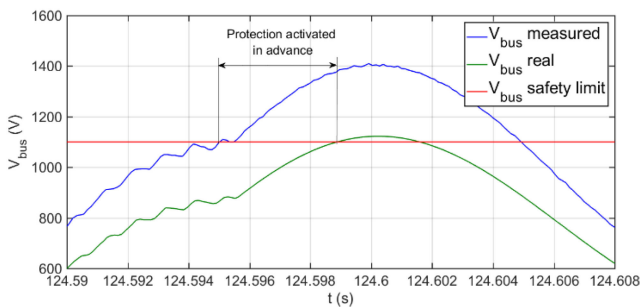


**Fig. 5** Comparison of braking chopper activation for DC-link sensor fault free a faulty cases

the catenary. Furthermore, the safety protection acts earlier, as it is shown in Fig. 5, decreasing the availability of the system.

Thus, gain faults are injected in the DC-link voltage sensor  $v_{bus}$ . Three scenarios for DC-link sensor are presented, one fault free and two faulty. The real torque per motor is shown in Fig. 6, based on an motor torque cycle of maximum positive torque (621 N m) and 1200 rpm, during 50 s, and maximum negative torque (565 N m) during 10 s. The current returned to the catenary is limited to 100 A.

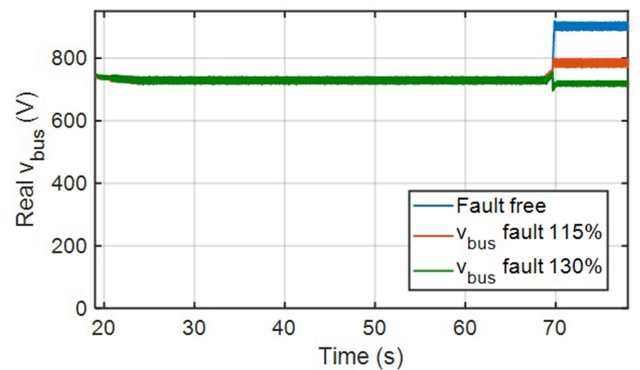


**Fig. 7** Real  $v_{bus}$  voltage for  $v_{bus}$  sensor fault scenarios

Real and measured  $v_{bus}$  are presented in Figs. 7 and 8, respectively. During the positive torque interval, the real  $v_{bus}$  is equal for the three scenarios, but the measured values are different. During the braking phase, and due to braking limits set as a function of measured DC-Link voltage values, the real values differ. In Fig. 9, the input power is shown. It can be seen that a voltage sensor measuring a higher value, generates an increase of the power dissipated in the crowbar, as Fig. 10 shows, decreasing the energy returned to the grid.

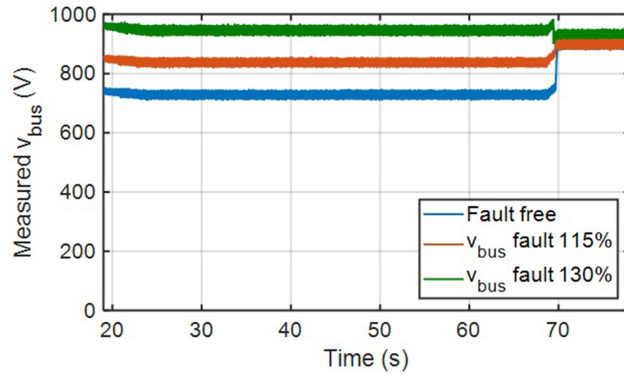


Fig. 8 Measured  $v_{bus}$  voltage for  $v_{bus}$  sensor fault scenarios

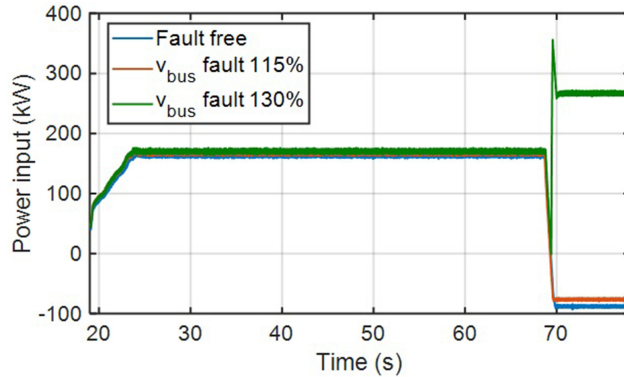


Fig. 9 Power input for  $v_{bus}$  sensor fault scenarios

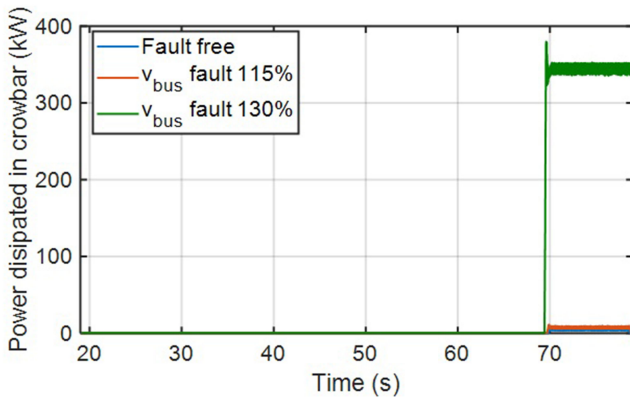


Fig. 10 Power dissipated in braking resistor for  $v_{bus}$  sensor fault scenarios

Moreover, a higher gain deviation, makes the input power positive during braking phase. It is assumed that only energy losses due to energy dissipated in braking resistor exist. Thus, the efficiency for the torque cycle proposed, in the fault-free scenario is 99.4%, whereas for the faulty scenarios, it decreases to 99.1% (15% deviation) and 69.6% (30% deviation). DC-link sensors measuring a higher value, up to 115%, do not suppose an important decrease of efficiency, but it is really important for higher gain faults. In Fig. 11, the measured  $i_{cat}$  is shown. During the traction phase the value for all the scenarios is similar, without important increases, a 115% gain fault supposes a 2% higher average  $i_{cat}$ , whereas a 130% gain fault a 3.8% increase, but during braking phase, very high  $i_{cat}$  can appear.

#### 4 Enhanced FMEA

The results shown in the previous section were obtained applying the methodology described in Section 2. Once the steps 1 to 4 have been developed in previous sections, the enhanced FMEA result is presented in this section.

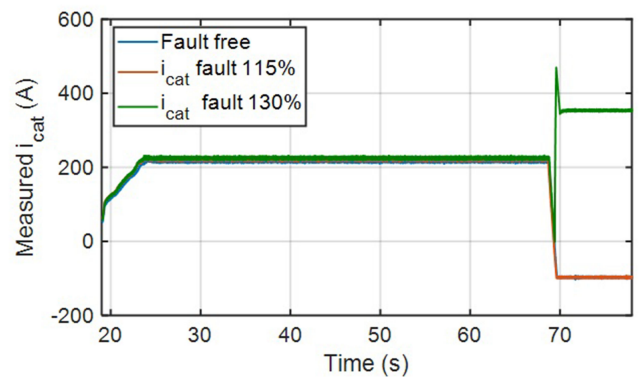


Fig. 11 Measured  $i_{cat}$  for  $v_{bus}$  sensor fault scenarios

The methodology can be repeated if new fault modes arise, but starting from the new enhanced FMEA. The main goal is to provide a continuous feedback to the FMEA during the system life cycle.

The cases analysed in this article, are presented in the enhanced FMEA in Table 3. A new column is added to the initial FMEA, presented in a reduced version in Table 1, and labelled as model-based system performance analysis.

The results presented should be an additional information to detect a sensor fault in the degraded mode. Based on the available enhanced FMEA, working point and the periodic variables captured, it is possible to detect a sensor fault effect, before failure occurs.

Furthermore, based on the performance analysis, it should be defined the most suitable maintenance action. It could be implemented as a visual tool, for example representing with different colours each level of degraded performance, so the maintenance expert takes a decision quickly. Thus, for example, an energy efficiency of 80% referred to the nominal one, can be represented by a yellow label, so it involves to analyse during the next periodic maintenance, whereas an energy efficiency of 60%, represented as orange label, it implies to order a maintenance

**Table 3** Enhanced FMEA

Sensor	Fault mode	Model-based system performance analysis
sensor $v_{bus}$	measured value higher than real one	<p><i>Motor working point: 621 N m, 1200 rpm. Braking 565 N m</i></p> <p>gain fault 115%:</p> <p>measured <math>i_{cat}</math> increases 2%</p> <p>real torque increases 1.6%</p> <p>efficiency (due to braking resistor losses) decreases from 99.38% to 99.09%</p> <p>gain fault 130%:</p> <p>measured <math>i_{cat}</math> increases 3.8%</p> <p>real torque increases 3.2%</p> <p>efficiency (due to braking resistor losses) decreases from 99.38% to 69.58%</p>
sensor $i_U$	measured value higher than real one	<p><i>motor working point: 460 N m and 600 rpm.</i></p> <p>gain fault 110%:</p> <p>jerk peak at <math>2f_s</math>: <math>10.69 \text{ m/s}^3</math>, increment of 51% related to fault free scenario.</p> <p>real torque decrease 9.6%</p> <p><math>i_U</math> and <math>i_V</math> measurements difference up to 6.7%</p> <p>gain fault 120%:</p> <p>Jerk peak at <math>2f_s</math>: <math>12.86 \text{ m/s}^3</math>, increment of 81% related to fault free scenario.</p> <p>real torque decrease 18.4%</p> <p><math>i_U</math> and <math>i_V</math> measurements difference up to 11.2%</p>

action. The level of performances should be set with design and maintenance teams from system manufacturer.

## 5 Conclusions

This work has presented the application of a methodology to generate an enhanced FMEA for sensor faults in a railway traction unit. The methodology is based on an initial FMEA from system manufacturer and a hardware-in-the-loop platform for fault injection and simulation. The system performance analysis enhances the FMEA, providing quantitative data. This data can be used to detect a sensor fault in the degraded zone and to take decision about the most suitable maintenance action.

## 6 References

- [1] Kara-Zaitri, C., Keller, A.Z., Barody, I., *et al.*: 'An improved FMEA methodology'. 1991 Proc. Annual Reliability and Maintainability Symp., Orlando, USA, 1991, pp. 248–252
- [2] Arabian-Hoseynabadi, H., Oraee, H., Tavner, P.J.: 'Failure modes and effects analysis (FMEA) for wind turbines', *Int. J. Electr. Power Energy Syst.*, 2010, **32**, (7), pp. 817–824
- [3] Colli, A.: 'Failure mode and effect analysis for photovoltaic systems', *Renew. Sustain. Energy Rev.*, 2015, **50**, pp. 804–809
- [4] Liu, H.-C., Liu, L., Liu, N.: 'Risk evaluation approaches in failure mode and effects analysis: a literature review', *Expert Syst. Appl.*, 2013, **40**, (2), pp. 828–838
- [5] Braaksma, A.J.J., Meesters, A.J., Klingenberg, W., *et al.*: 'A quantitative method for failure mode and effects analysis', *Int. J. Prod. Res.*, 2012, **50**, (23), pp. 6904–6917
- [6] del Olmo, J., Poza, J., Garramiola, F., *et al.*: 'Model driven hardware-in-the-loop fault analysis of railway traction systems'. 2017 IEEE Int. Workshop of Electronics, Control, Measurement, Signals and their Application to Mechatronics (ECMSM), Donostia-San Sebastian, Spain, 2017, pp. 1–6
- [7] Yang, C., Yang, C., Peng, T., *et al.*: 'A fault-injection strategy for traction drive control systems', *IEEE Trans. Ind. Electron.*, 2017, **PP**, (99), pp. 1–1
- [8] Sarhadi, P., Yousefpour, S.: 'State of the art: hardware in the loop modeling and simulation with its applications in design, development and implementation of system and control software', *Int. J. Dyn. Control*, 2015, **3**, (4), pp. 470–479
- [9] Isermann, R.: 'Fault-diagnosis systems' (Springer, Berlin, Heidelberg, 2006)
- [10] del Olmo, J.: 'Diagnóstico activo de unidades de tracción ferroviaria ante fallos en sensores', Mondragon Unibertsitatea, 2017
- [11] Aguirre, M., Calleja, C., Lopez-de-Heredia, A., *et al.*: 'FOC and DTC comparison in PMSM for railway traction application'. Proc. of the 2011 14th European Conf. on Power Electronics and Applications, Birmingham, UK, 2011, pp. 1–10
- [12] Aguirre, M., Poza, J., Aldasoro, L., *et al.*: 'Sensorless torque control of PMSMs for railway traction applications'. 2013 15th European Conf. on Power Electronics and Applications (EPE), Lille, France, 2013, pp. 1–10
- [13] Kwansup Lee, K.L., Jaechan Lee, J.L., Ilhwan Kim, I.K.: 'A study on strategy of condition based maintenance for Korea metro rolling stocks'. 7th IET Conf. on Railway Condition Monitoring (RCM 2016), Birmingham, UK, 2016, pp. 5 (4.)–5 (4.)
- [14] Marzat, J., Piet-Lahanier, H., Damongeot, F., *et al.*: 'Model-based fault diagnosis for aerospace systems: a survey', *Proc. Inst. Mech. Eng. G J. Aerosp. Eng.*, 2012, **226**, (10), pp. 1329–1360
- [15] Chung, D.-W., Sul, S.-K.: 'Analysis and compensation of current measurement error in vector controlled AC motor drives', *IEEE Trans. Ind. Appl.*, 1998, **34**, (2), pp. 340–345
- [16] ISO 2631-1(1997): 'Mechanical vibration and shock evaluation of human exposure to whole body vibration, part 1 general requirements' (International Organization for Standardisation, 1997, 2nd edn.)
- [17] 'EN 13452-1:2003 railway applications – braking-mass transit brake systems – part 1: performance requirements', 2003